JCB Article

The cysteine-rich domain regulates ADAM protease function in vivo

Katherine M. Smith,[1] Alban Gaultier,[1,2] Helene Cousin,[1] Dominique Alfandari,[1] Judith M. White,[1] and Douglas W. DeSimone[1]

[1]Department of Cell Biology, University of Virginia, Health Sciences Center, Charlottesville, VA 22908
[2]Laboratoire de Biologie Moléculaire et Cellulaire du Developpement, Université Pierre et Maire Curie, 75005 Paris, France

ADAMs are membrane-anchored proteases that regulate cell behavior by proteolytically modifying the cell surface and ECM. Like other membrane-anchored proteases, ADAMs contain candidate "adhesive" domains downstream of their metalloprotease domains. The mechanism by which membrane-anchored cell surface proteases utilize these putative adhesive domains to regulate protease function in vivo is not well understood. We address this important question by analyzing the relative contributions of downstream extracellular domains (disintegrin, cysteine rich, and EGF-like repeat) of the ADAM13 metalloprotease during *Xenopus laevis* development. When expressed in embryos, ADAM13 induces hyperplasia of the cement gland, whereas ADAM10 does not. Using chimeric constructs, we find that the metalloprotease domain of ADAM10 can substitute for that of ADAM13, but that specificity for cement gland expansion requires a downstream extracellular domain of ADAM13. Analysis of finer resolution chimeras indicates an essential role for the cysteine-rich domain and a supporting role for the disintegrin domain. These and other results reveal that the cysteine-rich domain of ADAM13 cooperates intramolecularly with the ADAM13 metalloprotease domain to regulate its function in vivo. Our findings thus provide the first evidence that a downstream extracellular adhesive domain plays an active role in regulating ADAM protease function in vivo. These findings are likely relevant to other membrane-anchored cell surface proteases.

Introduction

Proteolysis at the cell surface is a critical mediator of developmental processes, cellular homeostasis, and tissue repair, but can play deleterious roles in disease states. By cleaving ECM components and cell adhesion receptors, cell surface proteolysis can have profound effects on cell–matrix and cell–cell interactions. Proteolysis at the cell surface also accounts for ectodomain shedding, the process of cleaving latent progrowth factors and cytokines to release active forms from cell membrane attachments.

Four classes of membrane-anchored cell surface proteases have been identified that participate in these cleavage events: membrane-type matrix metalloproteases (MT-MMPs),* ectopeptidases, meprins, and ADAMs (a disintegrin and metalloprotease) (Stocker and Bode, 1995; Bauvois, 2001). Most of these cell surface proteases are type I integral membrane proteins that contain additional domains downstream of their protease domains (Fig. 1). Some of these nonproteolytic ectodomain elements have been shown to serve adhesive functions in vitro (Overall, 2002). For example, the hemopexin domain of MT1-MMP, the cysteine-rich domain of dipeptidylpeptidase IV, and the disintegrin and/or cysteine-rich domain of *Xenopus* ADAM13 have been shown, in in vitro biochemical experiments, to interact with ECM components such as collagen and fibronectin (De Meester et al., 1999; Seiki, 1999; Gaultier et al., 2002). The disintegrin domains of several ADAMs have also been shown to support integrin-mediated cell adhesion (Takahashi et al., 2001; Bridges et al., 2002; Eto et al., 2002). Very little is known about the role of the cysteine-rich domain in overall ADAM function. One recent in vitro study reported that the cysteine-rich domain of ADAM12 can interact with syndecans and mediate integrin-dependent cell spreading (Iba et al., 2000). Although various in vitro binding partners for these putative adhesive domains have been identified, it is not known if, or how, this binding might contribute to substrate selection and proteolytic function in vivo. We are investigating these fundamental questions for ADAM proteases.

Address correspondence to Dr. Douglas W. DeSimone, Department of Cell Biology, University of Virginia, Health Sciences Center, P.O. Box 800732, Charlottesville, VA 22908. Tel.: (434) 924-2172. Fax: (434) 982-3912. E-mail: dwd3m@virginia.edu

*Abbreviations used in this paper: BMP4, bone morphogenetic protein-4; kuz, kuzbanian; MT-MMP, membrane-type matrix metalloprotease; TIMP, tissue inhibitor of metalloproteases.

Key words: ADAM; metalloprotease; disintegrin; cysteine rich; *Xenopus*

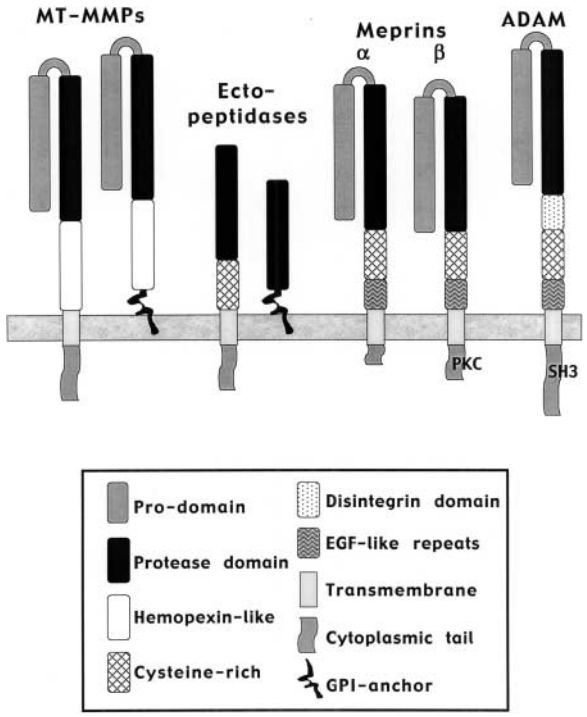

Figure 1. **Schematic representation of cell surface proteases.** Each is anchored in the membrane with a transmembrane domain or GPI linker. MT-MMPs and ectopeptidases come in both types, whereas meprins and ADAMs both possess transmembrane domains and cytoplasmic tails of varying sizes. Some ADAMs have SH3 ligand domains within their cytoplasmic tails. The cytoplasmic tails of meprin β subunits have a PKC phosphorylation site.

ADAM metalloproteases have been implicated in diverse developmental events such as fertilization, ECM remodeling, growth factor ectodomain shedding, and neurogenesis. ADAM proteases have a wide variety of substrates. They can degrade ECM components, shed cell-bound ectodomains to free growth factors and ligands from the cell surface, and cleave other integral membrane proteins (Blobel, 2000; Primakoff and Myles, 2000; Moss et al., 2001; Kheradmand and Werb, 2002). Through these mechanisms, ADAMs participate in cell migration, morphogenesis, tissue repair, and cell fate decisions. For the present study, we constructed chimeras between *Xenopus* ADAM10 and -13 in order to assess the contributions of the downstream, nonproteolytic domains to overall ADAM protease function in vivo. Although similarly structured, ADAMs 10 and 13 have different roles in development.

Xenopus ADAM13 is required for cranial neural crest cell migration, possibly by remodeling the fibronectin matrix en route (Alfandari et al., 2001). In addition to causing alterations in cranial neural crest morphology and behavior, overexpression of transcripts encoding ADAM13 results in hyperplasia of the cement gland (Cousin et al., 2000). The cement gland is the first ectodermally derived organ to differentiate in *Xenopus* embryos. It arises in the anteriormost part of the embryo and marks the dorsal–ventral axis boundary. Cement gland induction requires a gradient of the growth factor bone morphogenetic protein-4 (BMP4) as well as counter expression of its inhibitors such as noggin, follistatin, and chordin. Retinoic acid, eFGF, and Xwnt8 are also required to make a cement gland (Sive and Bradley, 1996). Many of these growth factors are first synthesized as membrane-tethered precursors and require extracellular proteolysis (shedding) to become active.

The *Drosophila* ADAM kuzbanian (kuz, also ADAM10) participates in axon extension through the ECM; kuz-null axons fail to form outgrowths (Fambrough et al., 1996; Schimmelpfeng et al., 2001). This failure of extension could be due to the matrix-degrading actions of kuz, or to its ability to bind and cleave ephrins (Ilan and Madri, 1999). Loss of kuz function in fly embryos results in perturbation of Notch signaling, which affects neurogenesis (Pan and Rubin, 1997; Lieber et al., 2002). Preliminary work in *Xenopus* suggests that ADAM10 plays a role in frog primary neurogenesis as well (Pan and Rubin, 1997). X-ADAM10 mRNA is expressed maternally throughout the embryo and then later becomes restricted to a pan-neural expression pattern (Pan and Rubin, 1997). As shown here, ADAM10 transcripts are also detected in the developing cement gland before its maturation. Although overexpression of wild-type ADAM10 message alters neural development, it has no affect on the genesis of the cement gland.

From our analyses of chimeras encoding domains of ADAMs 10 and 13, we find that the metalloprotease domain of either ADAM13 or ADAM10 is capable of inducing cement gland hyperplasia, but only if attached to the downstream adhesive domains of ADAM13. Further analyses indicate that the cysteine-rich domain of ADAM13 is absolutely essential to induce ectopic, expanded cement glands and, moreover, a disintegrin domain is required to support this behavior. Our data indicate that the cysteine-rich domains of ADAMs are important players in the biology of ADAM proteases in vivo. By extension, the nonproteolytic extracellular adhesive domains of other cell surface proteases (MT-MMPs, ectopeptidases, and meprins) may play similar roles.

Results

X-ADAM10 contains an extended HEXGH box sequence found in active metalloproteases

Xenopus ADAM10 was cloned by homology PCR using degenerate primers based on the sequence of *Drosophila* kuz and bovine ADAM10. A 1-kbp product was amplified from stage-34 *Xenopus* cDNA. Once the identity was confirmed by sequence analysis, a *Xenopus* stage-45 cDNA library was screened using the PCR fragment. Two X-ADAM10 clones of 2.5 kbp and 3 kbp were isolated. Each clone contained 3′ UTRs, but lacked the 5′ end. A *Xenopus* stage-17 cDNA library was screened using the larger clone in order to obtain a full-length cDNA. This screen yielded eight additional X-ADAM10 cDNAs, several of which contained the entire ADAM10 coding sequence. The full-length cDNA clone (GenBank/EMBL/DDBJ accession no. AF508151) has high sequence similarities with other ADAM10 family members: 80% identity with both bovine and human ADAM10 and 27% identity with *Drosophila* kuz. The *Drosophila* genome contains two *kuz/ADAM10* genes

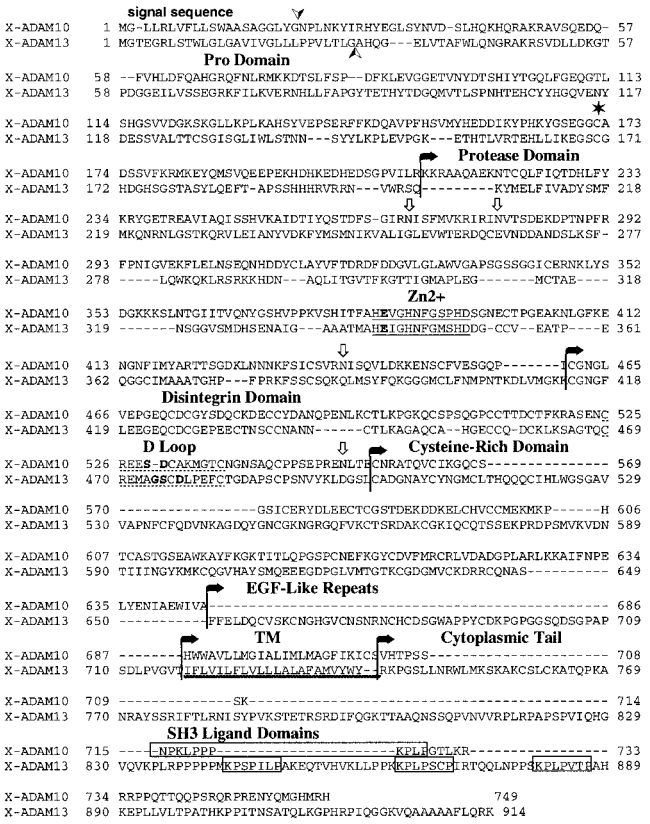

Figure 2. **Sequence comparison of X-ADAM10 and X-ADAM13.** Amino acid sequence alignments of full-length ADAM10 (GenBank/EMBL/DDBJ accession no. AF508151) and ADAM13 (accession no. U66003) with domain boundaries in black. The putative signal sequences are shown with an arrowhead. The cysteine-switch cysteine is indicated by a star (★) and all potential N-linked glycosylation sites in ADAM10 are denoted with an open arrow (⇓). The metalloprotease active site is underlined by a solid black line, the disintegrin loop is underlined by a broken line, and the transmembrane (TM) domain is underlined with a wavy line. All putative SH3 binding sites in the cytoplasmic tails of ADAMs 10 and 13 are boxed. Mutated amino acids in the zinc binding site (ADAM13 E341 to A; ADAM10 E385 to A) and the disintegrin loop (ADAM10 S529 to A and D530 to A; ADAM13 G474 to A, S475 to A, and D477 to A) are highlighted in bold.

(GenBank/EMBL/DDBJ accession nos. AE003640 and AAF56926), which share high protein sequence similarities with X-ADAM10. Over the entire coding region *Xenopus* ADAM10 and -13 share 20% identity, although the metalloprotease domains alone are more similar (23% identity) than the disintegrin domains (18% identity) when compared separately (Fig. 2). The sequence of X-ADAM10 contains a predicted metalloprotease extended active site. ADAM10 also has one putative SH3 binding domain (NPKLPPPKPL) within its cytoplasmic tail (Fig. 2). A partial cDNA clone containing part of the disintegrin and cysteine-rich domains of *Xenopus* ADAM10 was reported previously (Pan and Rubin, 1997) and is 97% identical to the corresponding portion of the deduced full-length protein sequence reported here. This suggests that these two cDNAs represent distinct ADAM10 pseudoalleles, which are commonly obtained from libraries prepared from tetraploid species such as *X. laevis*.

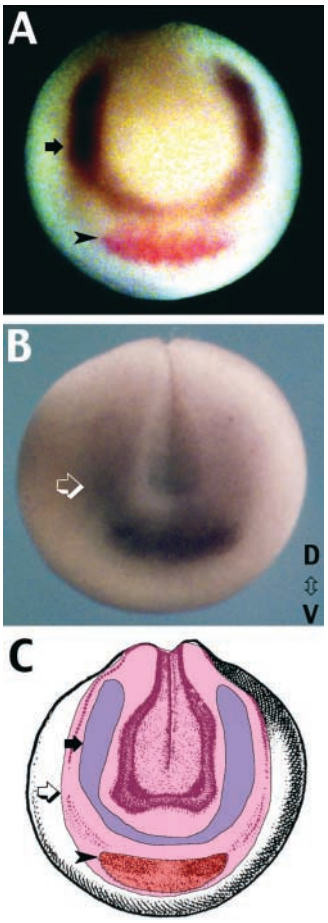

Figure 3. **Localization of ADAM13, ADAM10, and XCG mRNA in early *Xenopus* embryos.** (A) In an anterior view at stage 16, ADAM13 (purple, black arrow) mRNA is found in the neural crest and just dorsal to the cement gland anlagen (as marked by XCG mRNA expression in red, arrowhead), but the two transcripts do not overlap. (B) ADAM10 (light purple, open arrow) mRNA is localized to the entire neural plate and placodes, and encompasses the expression field of XCG. No distinct red color revealing XCG mRNA expression is seen because it is overlaid by the light purple ADAM10 costaining. (C) In a schematic of the *Xenopus* embryo at stage 16, the pink represents the entire neural plate and surrounding placodal and cement gland anlagen that express ADAM10 mRNA (open arrow). The ADAM10-expressing area encompasses both the regions of ADAM13 mRNA expression (blue, black arrow) and XCG (red, arrowhead) (Nieuwkoop and Faber, 1994).

Overexpression of ADAM13, but not ADAM10, causes hyperplasia of the cement gland

ADAM13 mRNA expression directly abuts the cement gland primordium dorsally before its specification (Fig. 3) and, when misexpressed anteriorly, enlarges the field of cells that become cement gland (Cousin et al., 2000; Fig. 4 D). To investigate the role of ADAM13 in cement gland organogenesis, transcripts encoding wild-type ADAM13 were microinjected into one cell of a two-cell embryo (Fig. 4 A). The embryos were then allowed to recover and grow under observation. When ADAM13 transcripts are misexpressed anteriorly by injection into the animal pole region of the embryo, 33% of the embryos have dorsally expanded cement glands (Fig. 4 D). This hyperplasia is not seen when transcripts encoding ADAM13, with a point mutation in the catalytic ac-

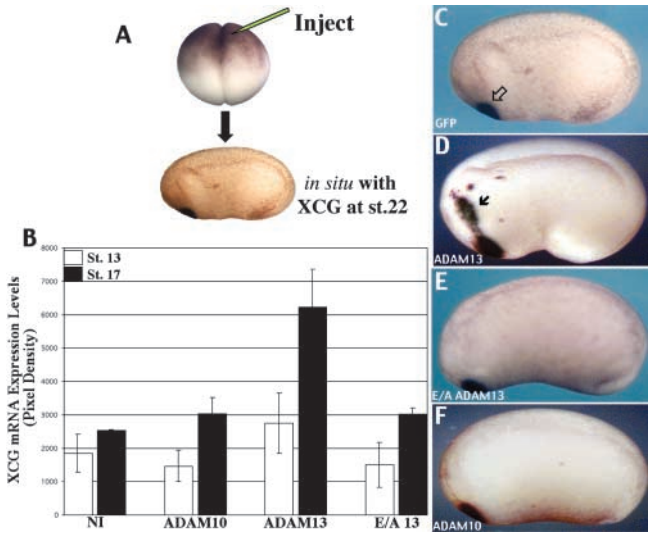

Figure 4. **Overexpression of wild-type ADAM13, but not ADAM10, results in hyperplasia of the cement gland.** (A) Transcripts encoding ADAM constructs are microinjected into the animal pole of one blastomere at the two-cell stage. The embryos are allowed to recover until stage 22^{+}, and then fixed for whole mount in situ hybridization with the cement gland marker XCG. (B) The increase in XCG mRNA levels caused by ADAM13 overexpression was quantified by RNA spot blot. Data are represented as relative values of expression based on average pixel densities obtained using the PhosphorImager. All levels of expression were within the linear range of this detection method. Data are shown as means ± SD of five independent experiments, each with pooled RNAs from 10 embryos. By stage 17, a twofold increase in XCG mRNA levels ($P < 0.05$) was found in embryos expressing ADAM13, but not E/A ADAM13 or ADAM10. The differences in XCG mRNA levels quantified by RNA spot blot were also observed by whole mount in situ hybridization. (C) GFP-injected embryos had no alterations in the cement gland marker XCG (black arrow), whereas large, ectopic islands of XCG-positive cells (D, arrow) were found when overexpressing ADAM13. Expression of the E/A ADAM13 mutant (E) or ADAM10 (F) had no affect on cement gland formation. NI, noninjected control; E/A13, E/A ADAM13.

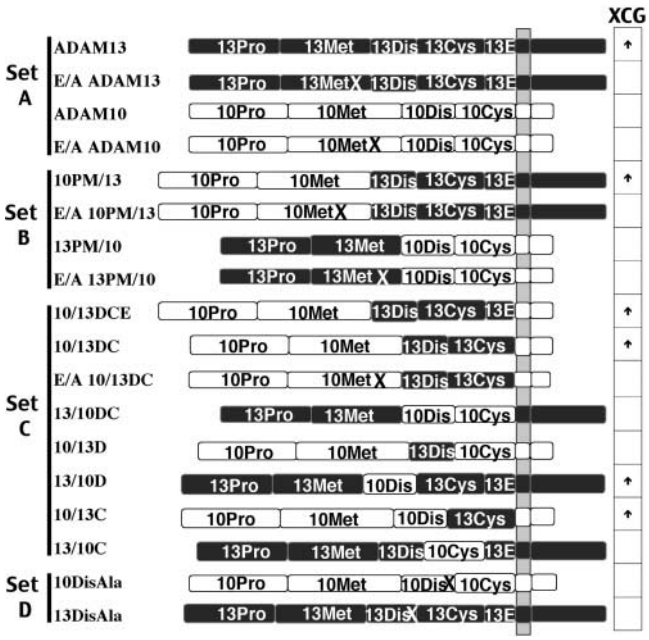

Figure 5. **Schematic representation of ADAM10 and -13 constructs.** Domains between ADAM10 (white) and ADAM13 (black) were switched as units (Pro/Met and DC ± E) or as individual domains (D and C). Chimeras containing metalloprotease domains with the catalytically inactive E/A point mutation were made. Mutations were also made in the disintegrin loops of both ADAM10 and -13. All constructs have been myc tagged. Mutated domains are denoted by an X. ADAM constructs that cause severe hyperplasia of the cement gland when ectopically expressed are designated by an up arrow. Blank boxes in this chart indicate that the construct had no significant affect on the cement gland. Set A consists of the wild-type and E/A point mutant constructs of ADAM10 and -13. Chimeras are grouped into Set B, for pro and met domain swaps, and Set C, for disintegrin and cysteine-rich domain swaps. Set D groups the disintegrin loop alanine point mutations.

tive site, is injected (Fig. 4 E, E/A ADAM13). When the same animal pole injections were performed using transcripts for wild-type ADAM10 (Fig. 4 F), no alterations in the cement gland were observed. Alterations in the expression of the cement gland marker XCG were detected by XCG in situ hybridizations and quantified by RNA spot blot. By stage 17, embryos injected with ADAM13 mRNA express more XCG RNA than either noninjected embryos or embryos injected with ADAM10 or E/A ADAM13 (Fig. 4 B).

ADAM10/13 chimeras are processed and transported to the cell surface

Because overexpression of ADAM13, but not ADAM10, leads to enlargement of the cement gland, we were able to undertake a study of how specific domains of ADAM13 are involved in specifying this activity. To do this, we switched domains between ADAM10 and -13 individually or as units. The pro and metalloprotease domains (Pro/Met, PM) were substituted as a unit and contained either the wild-type sequence or an E to A mutation (denoted by an X) in the protease active site (Fig. 5). Point mutations were also made in the disintegrin loops of ADAMs 10 and 13 in order to investigate disintegrin domain contributions to overall ADAM function. The resulting constructs (Fig. 5) were injected into embryos and assayed for expression and prodomain removal. The constructs were organized into four sets (Fig. 5 and see Fig. 7, Sets A–D) to simplify discussion throughout the text. Set A was developed to test whether ADAM 13 protease activity is required for cement gland hyperplasia. Set B constructs were designed to investigate whether specificity of protease activity resides within the protease domain or, rather, within one or more downstream domains. Set C was used to evaluate the critical role of the cysteine-rich domain in specifying protease activity. Set D constructs established the role of the ADAM13 disintegrin loop in supporting biological activity. All chimeras were processed to a putative metalloprotease active form (met form) of the approximate expected size based on calculated molecular weights (Fig. 6 A–C, open arrows).

Western blots of whole embryo lysates injected with ADAM transcripts revealed that wild-type ADAM13 was present at lower levels compared with ADAM10, whereas all pro/met domain chimeras and E/A ADAM13 were present at levels comparable to ADAM10 (Fig. 6 A). All disintegrin and cysteine-rich (DC) domain chimeras (with or without the

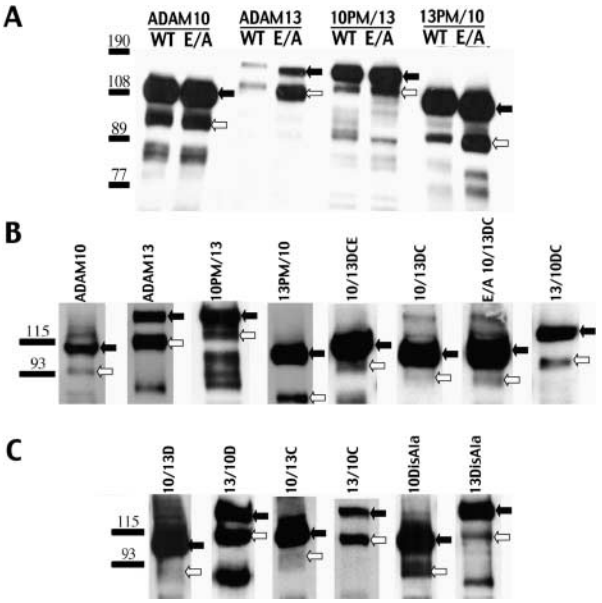

Figure 6. **All ADAM constructs are proteolytically processed and found on the cell surface.** (A) In whole embryo lysate Western blots with the anti–myc tag antibody, 9E10, both wild type and E/A mutants of ADAM10, ADAM13, and the Pro/Met chimeras are all found in unprocessed precursor forms with the pro-domain (black arrow) and in metalloprotease active forms, with the functionally repressive pro-domain removed (open arrows). (B and C) By affinity purification of cell surface biotin-labeled proteins and Western blotting with 9E10, the pro forms (black arrows) and metalloprotease forms (met forms, open arrows) of all ADAM constructs are seen. The pro and met forms generally run as expected based on calculated molecular weights with the addition of the myc tag.

EGF-like repeat; denoted by an E in Fig. 5) were also expressed and processed (Fig. 6, B and C; unpublished data). The same results were observed when the chimeric constructs were expressed in COS cells or the *Xenopus* cell line XTC (unpublished data). We next checked for cell surface expression of the constructs using a cell surface biotinylation protocol. Although endogenous ADAM13 is normally found on the surface only in its met form (Alfandari et al., 2001), here we observed both the pro (black arrows) and met (open arrows) forms on the surface (Fig. 6 B), likely due to overexpression. All ADAM chimeras and mutants were found on the surface in both pro and met forms (Fig. 6, B and C). Some of the met forms (those of 10PM/13, 13PM/10, 13/10DC, 13/10D, 13/10C, 13DisAla, and 10DisAla) were expressed at relatively high levels, whereas others (10/13DCE, 10/13DC, 10/13D, and 10/13C) were expressed at lower levels.

Although relatively low levels of the met form of 10/13DC were present at the cell surface, this chimera had potent cement gland–inducing activity (Fig. 7, Set C; Fig. 8 D); therefore, the quantity of met form present did not correlate with function over the range of concentrations used in these studies. In addition, the relative amount of met form to pro form did not appear to influence activity. Chimera 10/13DC had a high pro to met ratio (Fig. 6 B), but still remains highly effective in inducing cement gland expansion. Consequently, an abundance of ADAM pro form on the cell surface did not inhibit the activity of the cleaved protease active form.

		Pro form/Met form kD	% Normal	% Mild	% Severe	XCG Induction	Cell Surface Expression
Set A	*ADAM13 N=82	123.3 / 96.9	67	0	33	↑	++
	*E/A ADAM13 N=51	123.3 / 96.9	98	2	0		++
	ADAM10 N=211	105.1 / 81.0	94	6	0		+
	E/A ADAM10 N=102	105.1 / 81.0	99	1	0		+
Set B	10PM/13 N=190	129.5 / 105.4	50	2	47	↑	++
	E/A 10PM/13 N=137	129.5 / 105.4	93	7	0		++
	13PM/10 N=210	98.9 / 72.5	94	6	0		++
	E/A 13PM/10 N=121	98.9 / 72.5	94	6	0		++
Set C	10/13DCE N=209	113.8 / 89.7	71	8	22	↑	+
	10/13DC N=224	108.7 / 84.6	54	5	41	↑	+[a]
	E/A 10/13DC N=100	108.7 / 84.6	63	25 / 7	7		+
	13/10DC N=108	114.6 / 88.2	75	14	11		++
	10/13D N=265	103.9 / 79.8	93	7	0		+
	13/10D N=412	124.5 / 98.1	47	21	32	↑	++
	10/13C N=148	109.9 / 85.8	35	35 / 4	27	↑	+
	13/10C N=222	118.5 / 92.0	52	34 / 8	6		++
Set D	13DisAla N=264	123.3 / 96.9	74	26	0		++
	10DisAla N=132	105.1 / 81.0	86	14	0		++

Figure 7. **Summary of ADAM10/13 construct expression in embryos.** The molecular weights in kD were calculated by MacVector software and include the addition of the six myc tags and predicted N-linked glycosylations. After in situ hybridization with XCG, embryos were scored for mild or severe cement gland perturbations. The embryos with mild phenotypes were subdivided into two classes, in some cases (shown with a back slash), defined as one to three small spots of ectopic XCG expression or three to four small spots accompanied by <10% expansion of the area of the main cement gland. Severe phenotypes had numerous large islands of ectopic cement gland or substantial expansions (>10%) of the existing cement gland. Up arrows indicate the ability of a construct to induce severe cement gland hyperplasia (corresponding to arrows in Fig. 5). Constructs with high levels of cell surface expression in the met form (as compared with ADAM13) have two pluses (++) and embryos with lower levels of met forms are given one plus (+). N, the number of embryos assayed. [a]Low cell surface expression, but robust activity. *Previously we reported separate experiments involving the coexpression of equal amounts of transcript (0.5 ng each) encoding wild-type and E/A ADAM13, which led to a marked reduction (62%) in cement gland hyperplasia. We conclude that E/A ADAM13 can function as a dominant-negative inhibitor of wild-type ADAM13 in the cement gland assay; the details are reported in Alfandari et al. (2001).

The protease domains of ADAM10 and -13 are functionally interchangeable for inducing cement gland hyperplasia

Chimeric ADAMs were injected into embryos and analyzed for XCG expression at stages 20–24 of development. Em-

bryos were scored for mild or severe cement gland expansion. The presence of an active metalloprotease site in ADAM13 was required for hyperplasia of the cement gland (Fig. 4, D and E; Cousin et al., 2000). Nevertheless, the ADAM13 metalloprotease domain itself was not required per se for expansion of XCG expression; strong hyperplasia was seen in 47% of embryos injected with a chimera in which the ADAM10 pro and met domains are followed by the disintegrin, cysteine-rich, EGF-like repeat, transmembrane, and cytoplasmic tail domains of ADAM13 (Fig. 7, Set B, 10PM/13). In contrast, embryos expressing the reciprocal chimera composed of ADAM13 pro and met domains in an ADAM10 background (13PM/10) did not have expanded cement glands (Fig. 7, Set B). As with wild-type ADAM13, cement gland expansion activity was abolished in the 10PM/13 chimera when an E to A point mutation was introduced into the active site of ADAM10 (Fig. 7, E/A 10PM/13). These observations indicate that a functional protease domain is needed for cement gland induction, but that specificity for function does not reside within the ADAM13 protease domain (Fig. 7, Set B). These findings indicate that a downstream domain of ADAM13 is necessary for specifying the cement gland hyperplasia phenotype.

The disintegrin and cysteine-rich domains of ADAM13 are critical for function

In an earlier study we demonstrated that coexpression of E/A ADAM13 with ADAM13 results in a marked reduction in cement gland hyperplasia compared with ADAM13 expression alone (Alfandari et al., 2001). Thus, we conclude that E/A ADAM13 acts as a dominant-negative inhibitor of ADAM13 protease activity. Our hypothesis is that it does so by competing with wild-type ADAM13 for access to substrate. This finding further implicates ADAM13 domains downstream of the metalloprotease in regulating protease activity and/or substrate selectivity. Therefore, we sought to determine which domain(s) downstream of the ADAM13 metalloprotease domain is necessary to confer the cement gland expansion phenotype. We ruled out the cytoplasmic tail as a possible contributing factor because mutants of ADAM13 in which the tail is deleted still give the expanded cement gland phenotype (Cousin et al., 2000). We therefore focused on the disintegrin, cysteine-rich, and EGF-like repeat domains. Replacing the disintegrin and cysteine-rich (DC) domains of ADAM10 with those of ADAM13, with and without the EGF-like repeat (E), resulted in 22% (for 10/13DCE) and 41% (for 10/13DC) of embryos displaying severe hyperplasia of the cement gland (Fig. 7, Set C). The reciprocal chimera, ADAM13 with the disintegrin and cysteine-rich domains of ADAM10 (13/10DC), showed less activity than wild-type ADAM13 and yielded only 11% of embryos with cement gland expansion (Fig. 7, Set C). Swapping disintegrin domains alone had no effect on the function of either ADAM10 or ADAM13 in cement gland expansion. From this set of data, we conclude that either the ADAM13 cysteine-rich domain alone or the disintegrin and cysteine-rich domains together are responsible for specifying the cement gland phenotype (Fig. 7, Set C).

To distinguish the effects of the disintegrin domain from those of the cysteine-rich domain, the cysteine-rich domains

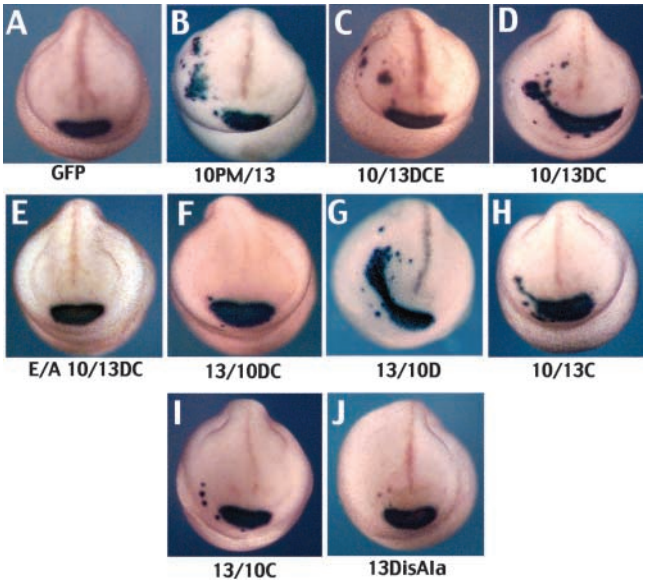

Figure 8. **Anterior views of representative stage-22 *Xenopus* embryos showing XCG mRNA expression.** (A) Embryos injected with GFP alone have no alterations in XCG expression. (B) Like ADAM13, the 10PM/13 chimeric construct causes a large expansion in XCG. The 10/13DCE (C) and 10/13DC (D) chimeras also perturb the cement gland. (E) An E/A point mutant in the catalytically active site of the 10/13DC chimera ablates its ability to cause hyperplasia of the cement gland. (F) Replacing ADAM13's disintegrin and cysteine-rich domains (chimera 13/10DC) did not fully ablate the XCG expansion, but it did lessen its severity. Replacing the disintegrin domain of ADAM13 with that of ADAM10 (chimera 13/10D) did not alter the function (G), whereas replacing only ADAM10's cysteine-rich domain with that of ADAM13 (10/13C) was sufficient to give that chimera the ability to cause alterations in XCG (H). Swapping ADAM13's cysteine-rich domain caused both a quantitative (6% severe phenotype vs. 33% for wild-type ADAM13; Fig. 7) and qualitative (I) decrease in activity. (J) Three point mutations in the disintegrin loop of ADAM13 diminish its ability to cause the enlargement of the cement gland, but do not affect its ability to cause its own degradation in vitro (unpublished data).

alone were swapped. A chimera in which the cysteine-rich domain of ADAM13 was placed in ADAM10 caused severe hyperplasia of the cement gland in 27% of embryos (Fig. 7, Set C, 10/13C; Fig. 8 H). Although the ADAM13 cysteine-rich domain alone in an ADAM10 background (10/13C) was sufficient to enable the chimera to expand the cement gland, the activity was more robust (41%) in a chimera containing both the disintegrin and cysteine-rich domains of ADAM13 (Fig. 7, Set C; Fig. 8, compare H with D).

Mutations designed to ablate disintegrin loop adhesive interactions in ADAM13 by replacing three critical amino acids with alanines (Bigler et al., 2000; Zhu et al., 2000; Takahashi et al., 2001) while keeping the protease domain intact (13DisAla) abolished cement gland expansion (Fig. 7, Set D; Fig. 8 J). Like wild-type ADAM13, the 13DisAla construct exhibited protease activity in an in vitro assay (unpublished data); therefore, mutating the disintegrin loop of ADAM13 does not destroy its inherent proteolytic capability. From this analysis we conclude that the ADAM10 and -13 disintegrin domains, although required, are functionally interchangeable in this system, but the cysteine-rich domains are functionally distinct and cannot compensate

for one another. Therefore, the cysteine-rich domain of ADAM13 is the major determinant specifying protease-dependent cement gland expansion.

Discussion

ADAMs are multidomain type I integral membrane proteins that are noted for their metalloprotease activities. They can function as sheddases to release active growth factors or cytokines (Blobel, 2000; Primakoff and Myles, 2000; Kheradmand and Werb, 2002), or they can cleave ECM components (Millichip et al., 1998; Alfandari et al., 2001; Schwettmann and Tschesche, 2001). Downstream of their metalloprotease domains, ADAMs contain three other domains that have been implicated as binding partners for other molecules in vitro. Many ADAM disintegrin domains support integrin-mediated cell adhesion (Evans, 2001; Takahashi et al., 2001; Bridges et al., 2002; Eto et al., 2002; White et al., 2002). The cysteine-rich domain of ADAM12 has been suggested to interact with syndecans and β1 integrins (Iba et al., 2000). In addition, the cytoplasmic tails of many ADAMs bind SH3 domain–containing ligands (Howard et al., 1999; Cousin et al., 2000; Kang et al., 2001). A major hypothesis has been that downstream domains affect protease function, for example, by helping to specify substrate recognition by the protease domain. Here we have used a robust activity of ADAM13, induction of cement gland hyperplasia in *Xenopus* embryos, to conduct a structure function analysis of the role of individual ADAM domains in a biological activity occurring in a developing organism.

For the present study we constructed a battery of chimeras containing domains of *Xenopus* ADAM13 and ADAM10. In contrast to ADAM13, ADAM10 does not induce cement gland hyperplasia. We found that the ADAM10 metalloprotease domain, however, could replace that of ADAM13 for this activity, indicating that substrate specificity does not lie within the ADAM13 metalloprotease domain. Conversely, a chimera containing the cysteine-rich domain of ADAM13 in an ADAM10 background was able to induce cement gland hyperplasia, indicating a key role for the cysteine-rich domain of ADAM13 in this activity. Two observations suggest that the disintegrin domain of ADAM13 also plays a supportive role. First, an ADAM10 chimera containing both the disintegrin and cysteine-rich domains of ADAM13 is a more potent inducer of cement gland hyperplasia (41% severe hyperplasia) than a chimera containing only the cysteine-rich domain (27% severe hyperplasia). Second, an ADAM13 mutant with alanine substitutions in its disintegrin loop does not induce cement gland hyperplasia. Collectively, our results suggest that both the disintegrin and cysteine-rich domains of ADAM13 are required for optimal induction of cement gland tissue. A previous in vitro chimeric analysis involving mammalian ADAM17 (TACE) and ADAM10 indicated a role for the "cysteine-rich domains" of ADAM17 for cleaving interleukin 1 receptor type II. However, because the prior study defined the "cysteine-rich domains" as a composite of the disintegrin and cysteine-rich domains of ADAM17, it did not resolve roles for the individual disintegrin or cysteine-rich domains (Reddy et al., 2000).

Model for intramolecular cooperation between cysteine-rich and metalloprotease domains

Three lines of evidence strongly suggest that the cysteine-rich domain of ADAM13 functions intramolecularly with the protease domain to specify cement gland hyperplasia. First, a chimera containing the ADAM10 metalloprotease domain followed by the disintegrin and cysteine-rich (DC) domains of ADAM13 (Fig. 7, Set C) is capable of inducing cement gland hyperplasia, whereas the same chimera with an E/A mutation in the protease domain is not. The same is true for wild-type and E/A ADAM13. Second, E/A ADAM13 functions as a dominant-negative to inhibit the ability of wild-type ADAM13 to produce cement gland expansion when both are coexpressed in the embryo (Alfandari et al., 2001). Our third line of support is a result of expressing a secreted soluble form of the ADAM13 disintegrin and cysteine-rich domains (DC). Soluble ADAM13 DC does not lead to any cement gland hyperplasia when expressed on its own, nor does it have any apparent dominant-negative effect on expressed wild-type ADAM13 in the cement gland assay (unpublished data). We therefore conclude that the cement gland hyperplasia phenotype is a direct result of intramolecular cooperation between the protease domain and the cysteine-rich domain of ADAM13 and not a result of either domain acting alone, in trans.

Model for involvement of the cysteine-rich domain in selecting ADAM protease substrates

We propose that by using its cysteine-rich domain, the ADAM13 metalloprotease attains a higher level of specificity or activity in cleaving a substrate(s) that is involved in cement gland induction. A simple model to explain our observations is that the cysteine-rich domain of ADAM13 binds to a site on the protease substrate, thereby facilitating cleavage. As discussed below, we consider it most likely that ADAM13 acts as a sheddase to induce cement gland hyperplasia. Hence the substrate could be a progrowth factor. Alternatively, the ADAM13 cysteine-rich (and disintegrin) domain(s) may bind to other receptors that, in turn, help select the ADAM13 substrate. Such alternate receptors could include integrins (Zhang et al., 1998; Eto et al., 2002; Bridges et al., 2002), syndecans (Iba et al., 2000), or ECM components (Gaultier et al., 2002). However, if the disintegrin domain of ADAM13 interacts with an integrin to induce cement gland hyperplasia (or other proteolytic functions), it is likely that the disintegrin domain–integrin interaction is not highly specific. In contrast, the cysteine-rich domain of ADAM13 is essential for conferring the ability of the ADAM13 metalloprotease domain to induce cement gland tissue. We therefore propose that the cysteine-rich domain is the key domain of ADAM13 involved in acting on a substrate, the cleavage of which initiates cement gland hyperplasia.

The model proposed above suggests that ADAM13 acts as a sheddase to induce cement gland hyperplasia. Related models can be invoked for processes involving ADAM-mediated cleavage of ECM substrates. ADAM13 can cleave fibronectin and can remodel a fibronectin matrix, activities that are likely involved in promoting cranial neural crest cell migration (Alfandari et al., 2001). There may be binding

site(s) for the disintegrin and cysteine-rich domains of ADAM13 on fibronectin or on alternate receptors (e.g., integrins and syndecans) that help select or position fibronectin for cleavage. Recent data support the former possibility (although not excluding the latter). A construct containing the disintegrin and cysteine-rich domains of ADAM13 supports integrin-mediated cell adhesion and binds to the HepII domain of fibronectin in vitro (Gaultier et al., 2002).

An alternative, but not mutually exclusive, model for the role of the cysteine-rich domain of ADAM13 in regulating its protease activity invokes interactions with an endogenous inhibitor, such as a tissue inhibitor of metalloproteases (TIMP). TIMPs can bind to both the protease and/or hemopexin domains of MMPs to regulate their activity (Murphy et al., 1992; Baragi et al., 1994). A similar regulatory interaction may occur between some ADAMs and TIMPs (Amour et al., 2000; Lee et al., 2002). The regulation of ADAM10/13 chimera protease activity by the disintegrin and cysteine-rich domains may be a function of specific TIMP binding to those adhesive domains. If, for example, ADAM13 is less sensitive than ADAM10 to the inhibitory effects of TIMPs, replacing ADAM10's putative TIMP binding site (the cysteine-rich domain) with that of ADAM13 would create a chimera with greater proteolytic activity.

Model for ADAM-mediated cement gland induction

Our findings demonstrate that ectopic expression of ADAM13 leads to cement gland hyperplasia and this activity depends critically on the cysteine-rich domain. How might this occur? The ectoderm of the *X. laevis* embryo is patterned into nonneuronal versus neuronal tissue by a gradient of BMP4 (Dale and Wardle, 1999). The gradient is further refined by expression of soluble inhibitors of BMPs and by expression of other growth factors and morphogens (Dale and Jones, 1999). Domains of high BMP4 expression become specified as nonneuronal ectoderm. Mid-ranges of BMP4 give rise to a field of cells that will become cement gland. The cement gland field arises at the dorsal–ventral border and marks the anteriormost part of the embryo. Endogenous pro-cement gland signals are present in the dorsal mesoderm (Gammill and Sive, 2000) where ADAM13 message is found. Therefore, it is possible that ADAM13 is an endogenous effector of cement gland. Alternatively, ADAM13 may be mimicking another ADAM metalloprotease that is an endogenous effector of cement gland tissue.

If ADAM13 does play a role in the development of the cement gland, then it must do so early, potentially by affecting the BMP4 gradient itself or a cell's ability to perceive the gradient. We reached this conclusion because expression of ADAM13 does not alter the mRNA expression patterns of the known cement gland inducers xrx and otx2 (unpublished data). Otx2 can directly turn on the cement gland marker XCG, and overexpression of otx2 leads to ectopic cement gland tissue ventrally in areas competent to become cement gland, as specified by BMP4 (Gammill and Sive, 1997). In contrast, the cement glands observed in embryos overexpressing ADAM13 are expanded dorsally. Therefore, when misexpressed anteriorly, ADAM13 can expand the field of cells that are capable of responding to the endogenous otx2 signaling cascade without altering otx2 directly.

Summary

In conclusion, this paper reveals an essential role for the cysteine-rich domain of an ADAM in regulating protease activity in vivo. Since their discovery, ADAMs have been identified in a wide variety of cell types and tissues. Their ability to process growth factors and cell surface receptors and to remodel the ECM is required for normal embryonic development, and when ADAM behavior goes awry in adult tissue, disease states may occur. By elucidating the mechanism by which the disintegrin and cysteine-rich domains help an ADAM identify and cleave a target substrate, we will begin to understand how ADAMs and other cell surface proteases function in development and disease.

Materials and methods

Embryo culture

X. laevis eggs were fertilized and the resultant embryos were dejellied in 2% cysteine and cultured as previously described (Newport and Kirschner, 1982). Staging of embryos was according to Nieuwkoop and Faber (1994).

Cloning of *X. laevis* ADAM10

Degenerative RT-PCR was performed on stage-34 whole embryo cDNA using nested primer pairs based on regions of high similarity in the sequences of *Drosophila* kuz (GenBank/EMBL/DDBJ accession no. U60591) and *Bos taurus* MADM (accession no. Z21961). RT-PCR was performed using two rounds of amplification with primers kuz-s1, 5′-tg/a/t/ctac/tata/c/tcaa/gacg/a/t/cga-3′, and kuz-as2, 5′-aca/gtca/gcaa/gtag/a/t/ccg/a/t/cc/tg/ta/gaa-3′, for round one and primers kuz-s2, 5′-tgc/tc/ttg/a/t/cgcg/a/t/ctatgtg/a/t/cttc/tac-3′, plus kuz-as2 for round two. The 1-kbp product was cloned into the pCR2.1 TA cloning kit vector (Invitrogen) and used as a probe to screen an *X. laevis* st.45 cDNA library. The resulting partial cDNA clone from that screen was used to probe a *Xenopus* st.17 cDNA library in λgt10 (Kintner and Melton, 1987), from which a clone containing the entire coding region of X-ADAM10 was isolated.

Production of chimeric constructs and mutants

Chimeric constructs of ADAM10 and ADAM13 were initiated by PCR amplification of individual domains with the addition of unique restriction sites engineered within the primers. Pfu DNA polymerase (Strategene) or Vent DNA polymerase (New England Biolabs, Inc.) was used in order to ensure high fidelity of amplification. The PCR products were then purified and incubated with taq DNA polymerase (Promega) before being cloned into the pCRII-TOPO vector (TOPO TA cloning kit; Invitrogen). The subcloned domain(s) was then excised and ligated back into $pCS2^{+}$ in the desired order to produce each chimera listed in Fig. 4. Domains were broken down as in Alfandari et al. (1997), with the disintegrin, cysteine-rich, and EGF-like domains starting on a cysteine. Alanine mutations were made in the disintegrin loop of ADAM10 (aa 529, S to A, and aa 530, D to A) and ADAM13 (aa 474, G to A; aa 475, S to A; and aa 477, D to A) using the QuikChange site-directed mutagenesis kit (Stratagene) and the following primers: ADAM10 forward primer, 5′-tgtcgggaggaagctgcctgtgccaagatgggaa-3′; ADAM10 reverse primer, 5′-ttcccatcttggcacaggcagcttcctccgaca-3′; ADAM13 forward primer, 5′-tgccgggaaatggctgcagcctgtgccctccggaattct-3′; and ADAM13 reverse primer, 5′-agaattccggaagggcacaggctgcagccatttcccggca-3′. PCR conditions were as recommended by the manufacturer, with Pfu DNA polymerase and 10 ng DNA template. All chimeras were confirmed by sequencing.

Microinjection

All constructs were cloned into the pCS2-myc expression vector, linearized with Not I, and transcribed into capped RNA using SP6 RNA polymerase (Promega). The transcripts were then run through a ProbeQuant G-50 spin column (Amersham Biosciences) before being extracted with phenol/chloroform and precipitated with 2.5 volumes of EtOH and 0.1 volume of 3 M NaAc. The RNAs were then resuspended in water to a final concentration of 0.1 mg/ml. 1 ng of RNA was injected into the animal pole region of one blastomere at the two-cell stage. GFP transcripts were coinjected with the chimeras, and then the embryos were sorted for left or right expressers under an epifluorescence dissecting scope before fixation for in situ hybridization or extraction for Western blots to confirm expression of the chimeras by probing for the myc epitope.

RNA spot blots

Total RNA from 10 embryos at various stages was extracted as in Chomczynski and Sacchi (1987) with the addition of a LiCl precipitation. Half an embryo was then spotted onto a nylon membrane using the Schleicher & Schuell spot blot system according to the manufacturer's instructions. *XCG* (provided by H. Sive, Wellcome Trust, Cambridge, UK) [^{32}P]UTP-labeled RNA probes were transcribed using the Strip-EZ RNA probe synthesis and removal kit (Ambion). High stringency conditions were used for both prehybridization and hybridization. Prehybridization occurred in 50% formamide, 6× SSPE, 5× Denhardt's solution, 0.5% SDS, and 100 mg/ml sheared salmon sperm DNA for 1–2 h at 68°C. Hybridization with probe was performed in 50% formamide, 6× SSPE, 0.5% SDS, and 100 μg/ml sheared salmon sperm DNA for 24 h at 68°C. Blots were then washed in 1× SSPE/0.5% SDS two times at room temperature and in 0.1× SSPE/0.1% SDS two to three times at 68°C. The spot blots were exposed to a phosphor screen for 24–72 h and then quantified using ImageQuant software (IQ Mac v1.2). The intensity of the RNA spots was analyzed for pixel density, with darker spots having more RNA and therefore higher density of pixels. Each sample was within the linear range of detection using storage phosphor technology (Johnston et al., 1990).

Whole mount in situ hybridization

Whole mount in situ hybridization on *X. laevis* embryos was performed as described by Harland (1991) with a few modifications (Cousin et al., 2000). Digital image acquisition of the embryos was undertaken in 1× PBS + 0.1% Tween-20 under a dissecting scope, using a Kodak DCS420c digital camera controlled with an Adobe Photoshop® plug-in (Kodak). Whole mount in situ hybridizations with the cement gland–specific probe XCG were done on all embryos injected with ADAM constructs to ensure that expansions of the cement gland were scored accurately.

Protein extraction and analysis

After injecting capped RNA transcripts into the embryo and allowing the embryos to neurulate, groups of 10 embryos were frozen on dry ice and then solubilized with 200 ml cold embryo solubilization buffer or ESB (100 mM NaCl, 50 mM Tris-HCl, pH 7.5, 1.0% Trition X-100, 2 mM PMSF, 5 mM EDTA). The cellular debris was pelleted by centrifugation at 14,000 rpm for 10 min at 4°C. Extraction with 300 ml of freon removed lipids from the supernatant, to which an equal volume of 2× laemmli with β-mercaptoethanol was added before boiling for 5 min and running on a 7% SDS-PAGE. Proteins were transferred to nitrocellulose membranes (Scleicher & Schuell) before Western blotting with the anti–myc tag antibody 9E10 (Santa Cruz Biotechnology, Inc.). To analyze cell surface expression, stage 15–16 injected embryos were biotinylated with EZ-Link sulfo-NHS-biotin (Pierce Chemical Co.) as previously described (Alfandari et al., 1995). To ensure that only cell surface proteins were biotinylated, control duplicate immunoprecipitation/Western blots were performed with an antibody to the cytoplasmic protein tubulin.

We thank Dr. Bette Dzamba for her critical reading of the manuscript.

This work was supported by United States Public Health Service grants HD26402 and DE014365 to D.W. DeSimone and GM48739 to J.M. White. A. Gaultier was supported, in part, by a grant from the Ministère de la Recherche et de la Technologie (99750). K. Smith was supported by National Institutes of Health training grant HL07284-21.

Submitted: 5 June 2002
Revised: 18 October 2002
Accepted: 28 October 2002

References

Alfandari, D., C.A. Whittaker, D.W. DeSimone, and T. Darribere. 1995. Integrin αv subunit is expressed on mesodermal cell surfaces during amphibian gastrulation. *Dev. Biol.* 170:249–261.

Alfandari, D., T.G. Wolfsberg, J.M. White, and D.W. DeSimone. 1997. ADAM 13: a novel ADAM expressed in somatic mesoderm and neural crest cells during *Xenopus laevis* development. *Dev. Biol.* 182:314–330.

Alfandari, D., H. Cousin, A. Gaultier, K. Smith, J.M. White, T. Darribere, and D.W. DeSimone. 2001. *Xenopus* ADAM 13 is a metalloprotease required for cranial neural crest cell migration. *Curr. Biol.* 11:918–930.

Amour, A., C.G. Knight, A. Webster, P.M. Slocombe, P.E. Stephens, V. Knauper, A.J. Docherty, and G. Murphy. 2000. The in vitro activity of ADAM-10 is inhibited by TIMP-1 and TIMP-3. *FEBS Lett.* 473:275–279.

Baragi, V.M., C.J. Fliszar, M.C. Conroy, Q.Z. Ye, J.M. Shipley, and H.G. Welgus. 1994. Contribution of the C-terminal domain of metalloproteinases to binding by tissue inhibitor of metalloproteinases. C-terminal truncated stromelysin and matrilysin exhibit equally compromised binding affinities as compared to full-length stromelysin. *J. Biol. Chem.* 269:12692–12697.

Bauvois, B. 2001. Transmembrane proteases in focus: diversity and redundancy? *J. Leukoc. Biol.* 70:11–17.

Bigler, D., Y. Takahashi, M.S. Chen, E.A. Almeida, L. Osbourne, and J.M. White. 2000. Sequence-specific interaction between the disintegrin domain of mouse ADAM 2 (fertilin β) and murine eggs. Role of the α(6) integrin subunit. *J. Biol. Chem.* 275:11576–11584.

Blobel, C.P. 2000. Remarkable roles of proteolysis on and beyond the cell surface. *Curr. Opin. Cell Biol.* 12:606–612.

Bridges, L.C., P.H. Tani, K.R. Hanson, C.M. Roberts, M.B. Judkins, and R.D. Bowditch. 2002. The lymphocyte metalloprotease MDC-L (ADAM 28) is a ligand for the integrin α4β1. *J. Biol. Chem.* 277:3784–3792.

Chomczynski, P., and N. Sacchi. 1987. Single-step method of RNA isolation by acid guanidinium thiocyanate-phenol-chloroform extraction. *Anal. Biochem.* 162:156–159.

Cousin, H., A. Gaultier, C. Bleux, T. Darribere, and D. Alfandari. 2000. PACSIN2 is a regulator of the metalloprotease/disintegrin ADAM13. *Dev. Biol.* 227:197–210.

Dale, L., and C.M. Jones. 1999. BMP signalling in early *Xenopus* development. *Bioessays.* 21:751–760.

Dale, L., and F.C. Wardle. 1999. A gradient of BMP activity specifies dorsal-ventral fates in early *Xenopus* embryos. *Semin. Cell Dev. Biol.* 10:319–326.

De Meester, I., S. Korom, J. Van Damme, and S. Scharpe. 1999. CD26, let it cut or cut it down. *Immunol. Today.* 20:367–375.

Eto, K., C. Huet, T. Tarui, S. Kupriyanov, H.Z. Liu, W. Puzon-McLaughlin, X.P. Zhang, D. Sheppard, E. Engvall, and Y. Takada. 2002. Functional classification of ADAMs based on a conserved motif for binding to integrin α9β1: implications for sperm-egg binding and other cell interactions. *J. Biol. Chem.* 277:17804–17810.

Evans, J.P. 2001. Fertilin β and other ADAMs as integrin ligands: insights into cell adhesion and fertilization. *Bioessays.* 23:628–639.

Fambrough, D., D. Pan, G.M. Rubin, and C.S. Goodman. 1996. The cell surface metalloprotease/disintegrin kuzbanian is required for axonal extension in *Drosophila*. *Proc. Natl. Acad. Sci. USA.* 93:13233–13238.

Gammill, L.S., and H. Sive. 1997. Identification of otx2 target genes and restrictions in ectodermal competence during *Xenopus* cement gland formation. *Development.* 124:471–481.

Gammill, L.S., and H. Sive. 2000. Coincidence of otx2 and BMP4 signaling correlates with *Xenopus* cement gland formation. *Mech. Dev.* 92:217–226.

Gaultier, A., H. Cousin, T. Darribere, and D. Alfandari. 2002. ADAM13 disintegrin and cysteine-rich domains bind to the second heparin- binding domain of fibronectin. *J. Biol. Chem.* 277:23336–23344.

Harland, R.M. 1991. In situ hybridization: an improved whole-mount method for *Xenopus* embryos. *Methods Cell Biol.* 36:685–695.

Howard, L., K.K. Nelson, R.A. Maciewicz, and C.P. Blobel. 1999. Interaction of the metalloprotease disintegrins MDC9 and MDC15 with two SH3 domain-containing proteins, endophilin I and SH3PX1. *J. Biol. Chem.* 274: 31693–31699.

Iba, K., R. Albrechtsen, B. Gilpin, C. Frohlich, F. Loechel, A. Zolkiewska, K. Ishiguro, T. Kojima, W. Liu, J.K. Langford, et al. 2000. The cysteine-rich domain of human ADAM 12 supports cell adhesion through syndecans and triggers signaling events that lead to β1 integrin-dependent cell spreading. *J. Cell Biol.* 149:1143–1156.

Ilan, N., and J.A. Madri. 1999. New paradigms of signaling in the vasculature: ephrins and metalloproteases. *Curr. Opin. Biotechnol.* 10:536–540.

Johnston, R.F., S.C. Pickett, and D.L. Barker. 1990. Autoradiography using storage phosphor technology. *Electrophoresis.* 11:355–360.

Kang, Q., Y. Cao, and A. Zolkiewska. 2001. Direct interaction between the cytoplasmic tail of ADAM 12 and the Src homology 3 domain of p85α activates phosphatidylinositol 3-kinase in C2C12 cells. *J. Biol. Chem.* 276:24466–24472.

Kheradmand, F., and Z. Werb. 2002. Shedding light on sheddases: role in growth and development. *Bioessays.* 24:8–12.

Kintner, C.R., and D.A. Melton. 1987. Expression of *Xenopus* N-CAM RNA in ectoderm is an early response to neural induction. *Development.* 99:311–325.

Lee, M.H., V. Verma, K. Maskos, J.D. Becherer, V. Knauper, P. Dodds, A. Amour, and G. Murphy. 2002. The C-terminal domains of TACE weaken the inhibitory action of N-TIMP-3. *FEBS Lett.* 520:102–106.

Lieber, T., S. Kidd, and M.W. Young. 2002. *kuzbanian*-mediated cleavage of

Drosophila Notch. *Genes Dev.* 16:209–221.

Millichip, M.I., D.J. Dallas, E. Wu, S. Dale, and N. McKie. 1998. The metallodisintegrin ADAM10 (MADM) from bovine kidney has type IV collagenase activity in vitro. *Biochem. Biophys. Res. Commun.* 245:594–598.

Moss, M.L., J.M. White, M.H. Lambert, and R.C. Andrews. 2001. TACE and other ADAM proteases as targets for drug discovery. *Drug Discov. Today.* 6:417–426.

Murphy, G., F. Willenbrock, R.V. Ward, M.I. Cockett, D. Eaton, and A.J. Docherty. 1992. The C-terminal domain of 72 kDa gelatinase A is not required for catalysis, but is essential for membrane activation and modulates interactions with tissue inhibitors of metalloproteinases. *Biochem. J.* 283:637–641.

Newport, J., and M. Kirschner. 1982. A major developmental transition in early *Xenopus* embryos: I. characterization and timing of cellular changes at the midblastula stage. *Cell.* 30:675–686.

Nieuwkoop, P.D., and J. Faber. 1994. Normal Table of *Xenopus laevis* (Daudin). Garland Publishing, Inc., New York. 252 pp.

Overall, C.M. 2002. Molecular determinants of metalloproteinase substrate specificity: matrix metalloproteinase substrate binding domains, modules, and exosites. *Mol. Biotechnol.* 22:51–86.

Pan, D., and G.M. Rubin. 1997. Kuzbanian controls proteolytic processing of Notch and mediates lateral inhibition during *Drosophila* and vertebrate neurogenesis. *Cell.* 90:271–280.

Primakoff, P., and D.G. Myles. 2000. The ADAM gene family: surface proteins with adhesion and protease activity. *Trends Genet.* 16:83–87.

Reddy, P., J.L. Slack, R. Davis, D.P. Cerretti, C.J. Kozlosky, R.A. Blanton, D. Shows, J.J. Peschon, and R.A. Black. 2000. Functional analysis of the domain structure of tumor necrosis factor-α converting enzyme. *J. Biol. Chem.* 275:14608–14614.

Schimmelpfeng, K., S. Gogel, and C. Klambt. 2001. The function of leak and kuzbanian during growth cone and cell migration. *Mech. Dev.* 106:25–36.

Schwettmann, L., and H. Tschesche. 2001. Cloning and expression in *Pichia pastoris* of metalloprotease domain of ADAM 9 catalytically active against fibronectin. *Protein Expr. Purif.* 21:65–70.

Seiki, M. 1999. Membrane-type matrix metalloproteinases. *APMIS.* 107:137–143.

Sive, H., and L. Bradley. 1996. A sticky problem: the *Xenopus* cement gland as a paradigm for anteroposterior patterning. *Dev. Dyn.* 205:265–280.

Stocker, W., and W. Bode. 1995. Structural features of a superfamily of zinc-endopeptidases: the metzincins. *Curr. Opin. Struct. Biol.* 5:383–390.

Takahashi, Y., D. Bigler, Y. Ito, and J.M. White. 2001. Sequence-specific interaction between the disintegrin domain of mouse ADAM 3 and murine eggs: role of β1 integrin-associated proteins CD9, CD81, and CD98. *Mol. Biol. Cell.* 12:809–820.

White, J.M., D. Bigler, M. Chen, Y. Takahashi, and T.G. Wolfsbery. 2002. ADAMs. *In* Cell Adhesion: Frontiers in Molecular Biology. M. Beckerle, editor. Oxford University Press, Oxford. 189–216.

Zhang, X.P., T. Kamata, K. Yokoyama, W. Puzon-McLaughlin, and Y. Takada. 1998. Specific interaction of the recombinant disintegrin-like domain of MDC-15 (metargidin, ADAM-15) with integrin αvβ3. *J. Biol. Chem.* 273: 7345–7350.

Zhu, X., N.P. Bansal, and J.P. Evans. 2000. Identification of key functional amino acids of the mouse fertilin β (ADAM2) disintegrin loop for cell-cell adhesion during fertilization. *J. Biol. Chem.* 275:7677–7683.